

phepy: Visual Benchmarks and Improvements for Out-of-Distribution Detectors

Juniper Tyree, Andreas Rupp, Petri S. Clusius, and Michael H. Boy

Abstract—Applying machine learning to increasingly high-dimensional problems with sparse or biased training data increases the risk that a model is used on inputs outside its training domain. For such out-of-distribution (OOD) inputs, the model can no longer make valid predictions, and its error is potentially unbounded.

Testing OOD detection methods on real-world datasets is complicated by the ambiguity around which inputs are in-distribution (ID) or OOD. We design a benchmark for OOD detection, which includes three novel and easily-visualisable toy examples. These simple examples provide direct and intuitive insight into whether the detector is able to detect (1) linear and (2) non-linear concepts and (3) identify thin ID subspaces (needles) within high-dimensional spaces (haystacks). We use our benchmark to evaluate the performance of various methods from the literature.

Since tactile examples of OOD inputs may benefit OOD detection, we also review several simple methods to synthesise OOD inputs for supervised training. We introduce two improvements, *t*-poking and OOD sample weighting, to make supervised detectors more precise at the ID-OOD boundary. This is especially important when conflicts between real ID and synthetic OOD sample blur the decision boundary.

Finally, we provide recommendations for constructing and applying out-of-distribution detectors in machine learning.

Index Terms—Out-of-Distribution Detection, Visualisation, Explainable AI, Adversarial Machine Learning.

I. INTRODUCTION

IN machine learning, the closed-world assumption is generally assumed to hold. That is, it is assumed that a model’s in-distribution (ID) training data is drawn independently and identically distributed (iid) from the same distribution as the test data and the data on which the model is later applied [1]. However, this assumption is broken when the model is applied to new out-of-distribution (OOD) data, and the model’s predictions can no longer be trusted.

Detecting out-of-distribution inputs thus is a critical component of machine learning. This paper explores two crucial aspects of OOD detection: methods for identifying novel inputs (Section III) and techniques to synthesise OOD inputs for supervised training methods (Section IV). Thus, this paper aims to provide an overview and recommendations (Section V) for OOD detection, including several small improvements.

J. Tyree, P. S. Clusius, and M. H. Boy are with the Institute for Atmospheric and Earth System Research, University of Helsinki, Helsinki, Finland.

A. Rupp and M. H. Boy are with the LUT School of Engineering Sciences, LUT University, Lappeenranta, Finland.

Manuscript submitted on 27.07.2023.

II. RELATED WORK

The task of detecting individual OOD inputs is an application of **novelty**, outlier, or anomaly **detection**. In contrast, concept drift detection methods [2] can identify population-level shifts.

It is often assumed that a machine learning model should perform well on inputs that are close to the inputs it was trained on, even though embedded bias, noisy data, bad features, and overfitted models all break this assumption. For instance, the Mahalanobis distance can be used to define a hyper-ellipsoid bounding volume by assuming that the ID data comes from a multivariate normal distribution [3]. Since the feature distances on high-dimensional inputs are vulnerable to noise and difficult to interpret, the distances are often computed on higher-level and lower-dimensional embeddings, e.g. created by the upstream levels of a neural network [4].

Clustering-based algorithms are also commonly used to detect novel inputs. For instance, the local outlier factor (LOF) [5] estimates the local training data density. The LOF thus differentiates between areas of high density, which are ID, and areas with low density, where an input is likely OOD. Alternatively, if the input data points can be naturally assigned to a set of clusters, inputs that clearly belong to one cluster can be assumed to be ID. In contrast, the membership scores of OOD inputs approach a uniform distribution [6].

Auto-associative (neural) networks are trained to reconstruct inputs with minimal error after compressing them through a bottleneck layer [7]. When trained on ID data only, they learn to exploit its structure. Given OOD inputs, however, their learnt assumptions are broken, and reconstruction fails. Thus, the magnitude of the reconstruction error can be used to differentiate between ID and OOD inputs. Networks that use non-linear activation functions can fit any non-linear function “with support in the unit hypercube” [8] and implement truncated non-linear principal component analysis (PCA) [7].

Many OOD inputs are often semantically valid inputs missing from the training data, which are thus only OOD due to incomplete knowledge about the parameter space. Since they can be detected as having high epistemic uncertainty, existing (Bayesian) uncertainty quantification methods such as Monte Carlo Dropout [9], Deep Ensembles [10], and Gaussian Processes have often been applied. In addition, noise-contrastive priors have been used to ensure that (synthetic) OOD inputs are associated with high uncertainty [11].

Supervised OOD detectors can be used if training OOD inputs are given or can be synthesised to augment the training data. Pei, Zhang, Fan *et al.* [1], for instance, sample trivial OOD inputs uniformly from each training batch’s input range. They then optimise a Generative Adversarial Network (GAN) to detect ID inputs as ID but shuffled class labels and trivial OOD inputs as OOD. Next, synthetic ID inputs are sampled from the GAN’s generator and pushed towards OOD using the fast gradient sign method [12] with normal-distributed steps, thus producing increasingly difficult OOD inputs. Alternatively, the GAN can be trained to directly synthesise OOD inputs in regions with a low density of training data [13].

III. TOY-COMPARISONS OF OOD DETECTION METHODS

Evaluating OOD detectors is often difficult as the complexity of the data can obscure how a method performs. We introduce *phepy*, an open-source Python package to visually evaluate OOD detectors using three intuitive toy examples:

- 1) Two groups of training points are scattered along a line in the 2D feature space. The target output variable only depends on the location along the line. In this example, points off the line are definitely OOD.
- 2) The training points are scattered around the sine-displaced boundary of a circle, but none are inside it. The target output variable only depends on the location along the boundary. Again, points off the line are OOD.
- 3) The training points are sampled from a 10-dimensional multivariate normal distribution but one of the features is set to a constant. This example tests whether an OOD detector can find a needle in a haystack, i.e. identify that points which do not share the constant are OOD.

In the following figures, each row showcases one detector. Its detection score is transformed into a CET-L20-colour-coded [14] confidence level representing the percentage of validation data with greater or equal ID scores [4]. The first two plots depict a subset of the training points in unlabelled 2D feature space with black markers. The third plot instead shows the *distribution* of confidence values for different values for the constant-in-training feature. A white line marks this constant.

First, we compare one interpretation of an ideal OOD detector with one-class support vector machines (SVMs), an unsupervised method available in *sklearn* [15]. Figure 1 shows that while the ideal detector succinctly extracts the training data subspaces on the line and circle boundaries, the one-class SVM generates two blurry confidence hills on the line and wrongly classifies most of the full circle as ID. For the haystack, the ideal detector assigns high confidence only to inputs that share the constant feature seen in training. One-class SVM instead spreads its confidence values uniformly.

Figure 2 compares both distance- and uncertainty-based detectors. Unsurprisingly, the Mahalanobis distance fails on the circular example since a normal distribution cannot express this boundary. Identifying OOD inputs based on Gaussian Process uncertainty performs best across all three test cases but requires subsampling to keep the $O(N^3)$ method’s runtime low. The three other methods fail in the haystack example. Interestingly, using noise-contrastive priors with Gaussian processes worsens its precision for the line and haystack. Note also that all methods are conservative in the line example and only confident around the two training data groups.

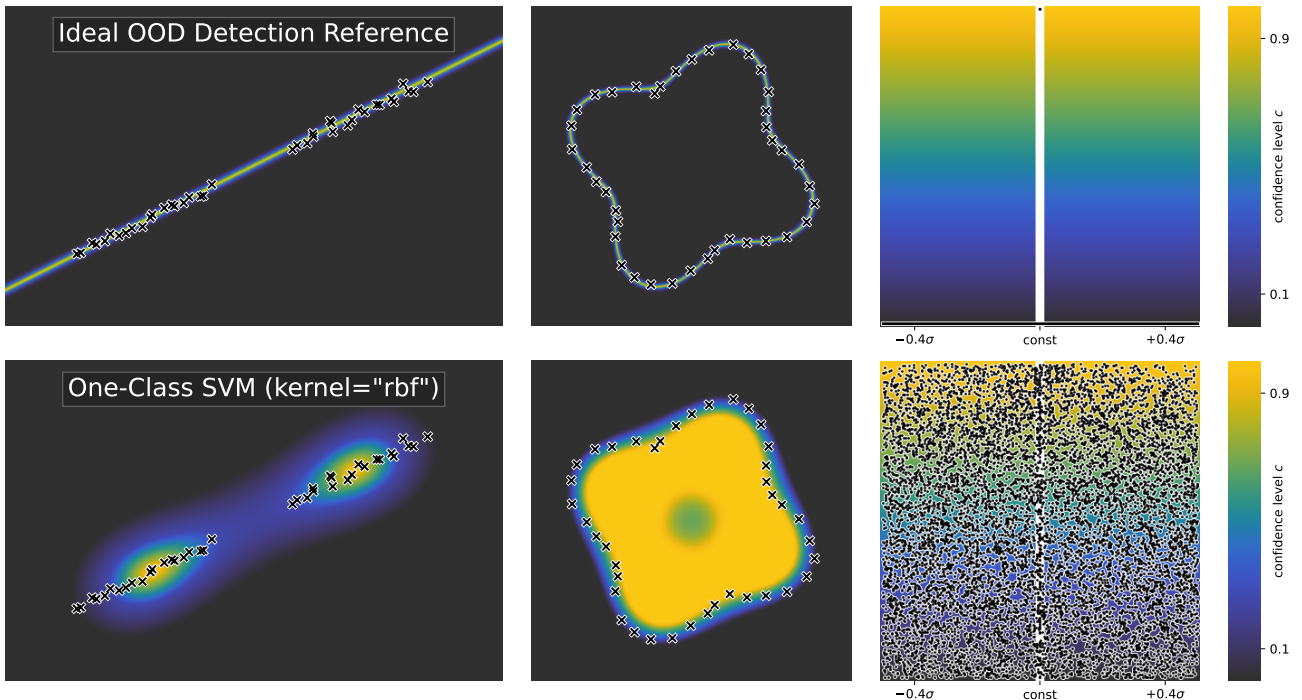


Figure 1. Comparison of the reference OOD detector and one-class SVM. Note that the reference is only one possible ideal detection method.

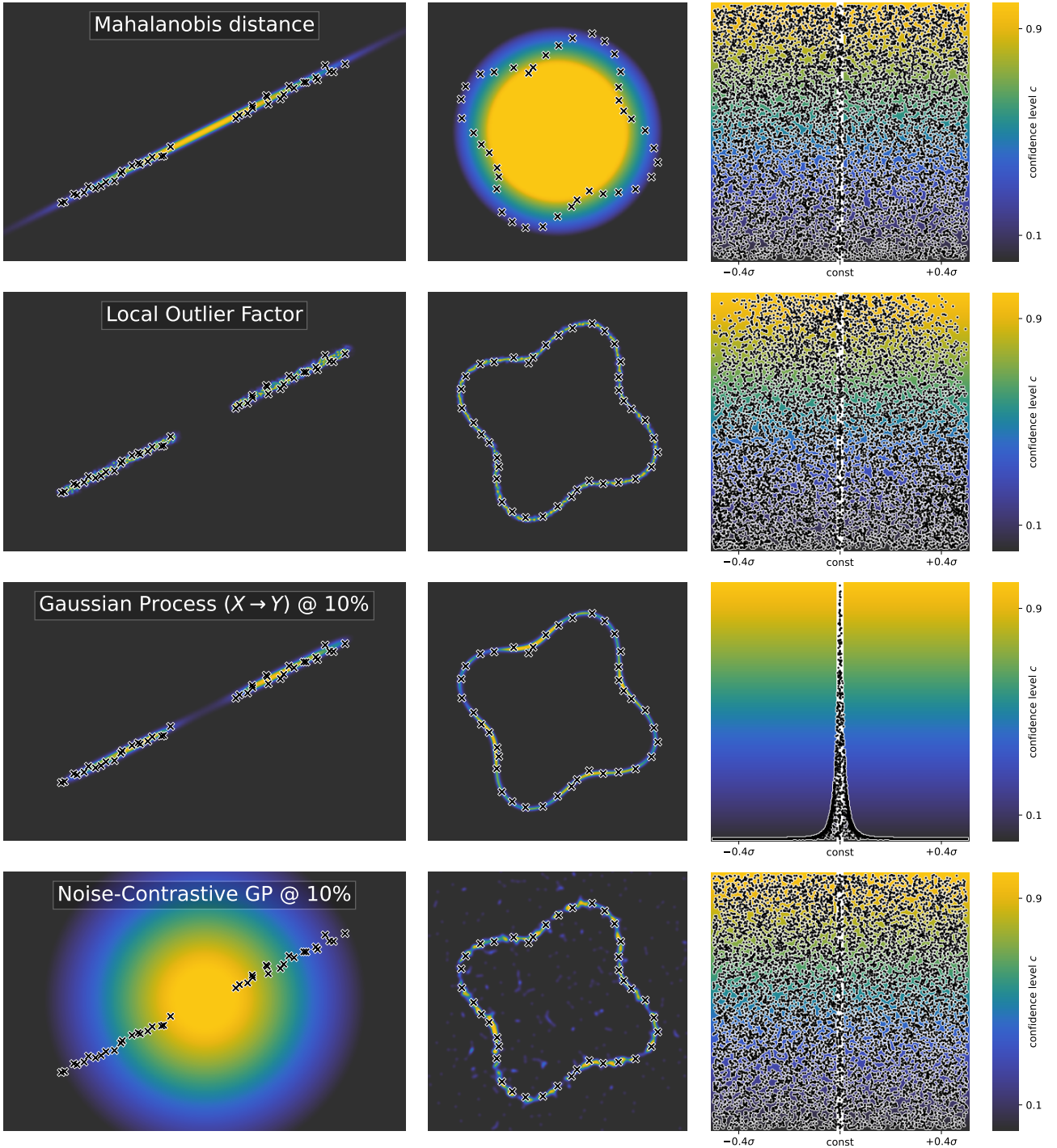


Figure 2. Comparison of the Mahalanobis distance, the Local Outlier Factor, Gaussian Processes, and Noise-Contrastive Priors as OOD detectors.

The auto-associative methods in Figure 3 all recognise that the haystack is not fully ID. The cheap truncated PCA and simple auto-associative multilayer perceptrons, which are constructed with $16 \times 1 \times 16$ hidden layer sizes, both display systematic problems if the sum of squared reconstruction errors is used as an OOD score. Taking the Mahalanobis distance of the errors instead improves the detection. Interestingly, auto-associative Gaussian processes (GPs) perform similarly to GPs that need more data and can thus provide higher performance.

In addition to the aforementioned qualitative evaluation, we also score each detector quantitatively. We decide to define points within two standard deviations off the line and circular boundary as well as points in the haystack with the seen-in-testing constant value as ID. We further calculate the true positive score as the sum of the ID scores for all test points that are truly ID. Table I shows each predictor's resulting precision, F_1 score, and the area under the receiver operating characteristic curve (ROC-AUC). We also measure the time

and memory required to fit each method and score each toy example's test data. All tests were performed on a Linux (6.1.91-060191-generic) machine with an AMD EPYC 7B13 (x86_64) processor with 8 physical and 16 total CPU cores and 62.79GiB of RAM.

In this section, we have introduced three reference toy examples to evaluate and compare different OOD detection methods, such that failure cases can be explained easily. We

make the following recommendations based on our experiments:

- 1) The Local Outlier Factor is efficient and works well for low-dimensional spaces without harsh OOD boundaries.
- 2) Gaussian Process uncertainty generalises well to all test cases but has high computational complexity.
- 3) Auto-associative networks identify the structural assumptions of the ID subspace. Applying the Mahalanobis distance to the reconstruction errors aids the detec-

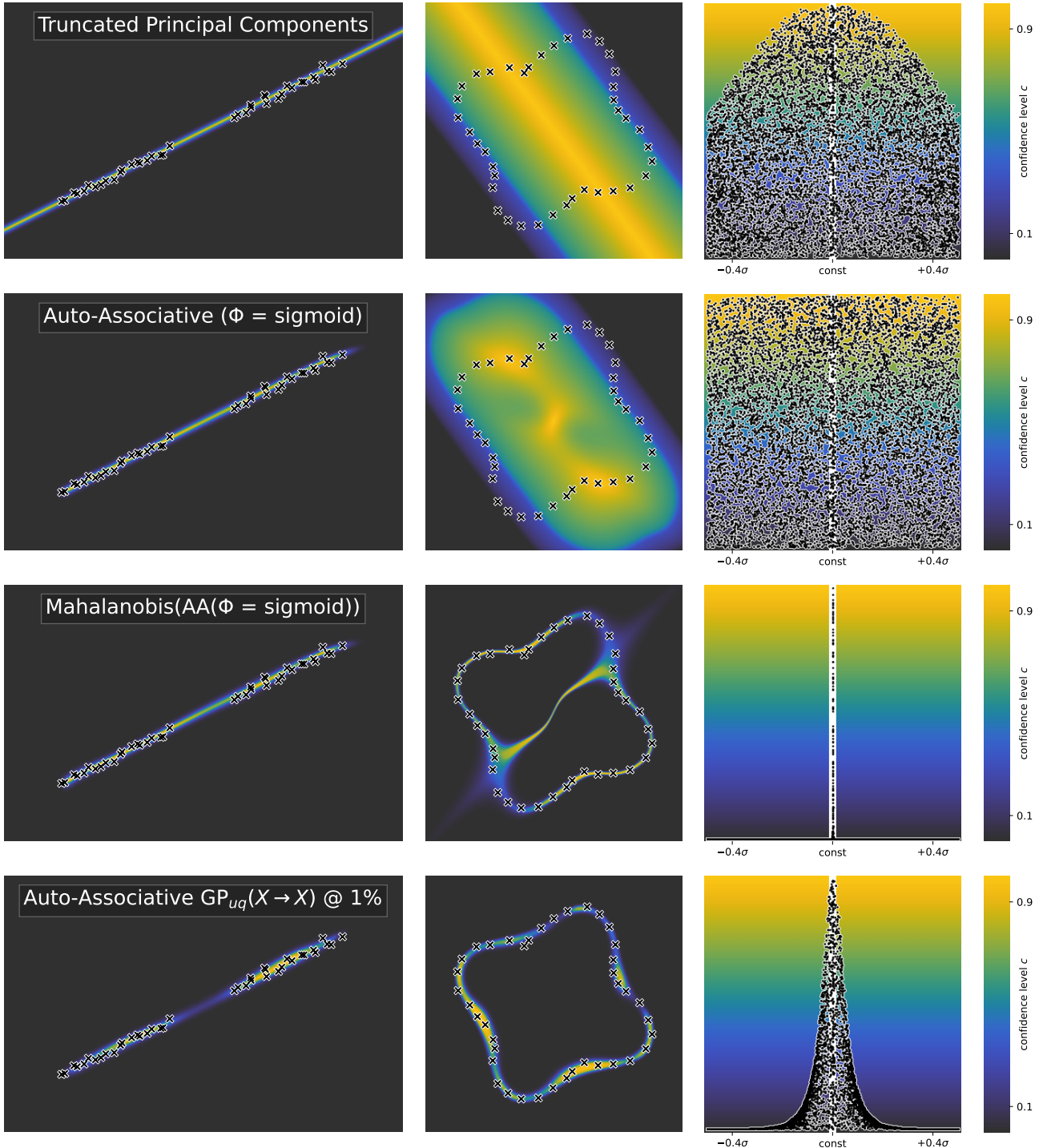


Figure 3. Comparison of truncated PCA, neural networks (sharpened by the Mahalanobis distance), and Gaussian Processes as auto-associative OOD detectors.

Table I
 QUANTITATIVE EVALUATION OF THE DETECTION, RUNTIME, AND MEMORY PERFORMANCE OF THE OOD DETECTORS FROM FIGURES 1 TO 3.

OOD Detector Toy Example	Precision	F ₁ Score	ROC-AUC	Fitting Time [s]	Scoring Time [s]	Memory [kiB]
	L / C / H	L / C / H	L / C / H	L / C / H	L / C / H	L / C / H
1a Reference	0.978 / 0.958 / 1.0	0.56 / 0.602 / 1.0	1.0 / 1.0 / 1.0	-	-	-
1b 1c-SVM	0.268 / 0.073 / 0.01	0.29 / 0.127 / 0.019	0.796 / 0.65 / 0.479	2.01 / 1.91 / 2.64	203 / 337 / 1.83	140 / 140 / 453
2a MD	0.974 / 0.072 / 0.009	0.514 / 0.124 / 0.018	0.999 / 0.637 / 0.455	0.0 / 0.0 / 0.0	0.05 / 0.11 / 0.0	0.63 / 0.63 / 2.19
2b LOF	0.967 / 0.94 / 0.011	0.398 / 0.61 / 0.022	0.827 / 0.999 / 0.558	0.04 / 0.03 / 0.56	6.16 / 10.2 / 0.57	426 / 426 / 1e3
2c GP @10%	0.965 / 0.92 / 0.168	0.395 / 0.599 / 0.249	0.878 / 0.998 / 0.967	3.23 / 5.97 / 5.2	600 / 1e3 / 0.5	8e3 / 8e3 / 8e3
2d nc-GP @10%	0.067 / 0.727 / 0.009	0.116 / 0.571 / 0.018	0.578 / 0.99 / 0.47	3.54 / 6.26 / 8.38	630 / 1e3 / 0.79	8e3 / 8e3 / 8e3
3a PCA-trunc.	0.978 / 0.056 / 0.012	0.561 / 0.1 / 0.024	1.0 / 0.502 / 0.59	0.02 / 0.0 / 0.0	1.48 / 0.71 / 0.1	1.36 / 1.35 / 1.37
3b Auto-Assoc.	0.961 / 0.064 / 0.01	0.449 / 0.113 / 0.02	0.891 / 0.567 / 0.503	4.33 / 2.56 / 1.86	1.38 / 2.14 / 0.1	19.3 / 16.8 / 21.3
3c MD(AA)	0.937 / 0.49 / 0.892	0.446 / 0.469 / 0.611	0.876 / 0.971 / 0.999	4.59 / 3.29 / 2.2	1.59 / 2.49 / 0.01	19.8 / 17.3 / 23.3
3d AA-GP @1%	0.897 / 0.612 / 0.062	0.417 / 0.54 / 0.109	0.877 / 0.981 / 0.914	0.89 / 0.75 / 2.46	14.2 / 21.7 / 0.3	88.3 / 88.3 / 107

tion, which truncated PCA can cheaply approximate.

IV. TOY-COMPARISONS OF OOD SYNTHESIS METHODS

Section III has examined several unsupervised OOD detection methods, which are trained using only ID samples. However, tasks such as providing meaningful OOD confidence scores benefit from being trained with both ID and OOD samples. This section evaluates several simple approaches to synthesising OOD inputs given the ID input points. First, we train a multi-layer perceptron classifier on the ID and synthetic OOD inputs using the default settings in `sklearn` [15] and take its prediction probability as its confidence. We again use the three toy examples from Section III to evaluate the final detector’s performance, which reflects the synthesis method’s quality. To visualise the OOD synthesiser’s performance, the line and circle plots now show synthetic OOD points as white dots.

Sampling random noise is a commonly used technique to synthesise OOD inputs [1], [11], [13]. The first row of Figure 4 shows that uniform OOD inputs [1] already produce reasonable OOD boundaries for the line and circle. However, OOD and ID inputs are not prevented from overlapping, and the detector thus fails to separate OOD inputs in the haystack.

Adversarial methods provide a more targeted approach to generating OOD inputs. We test the Fast Gradient Sign Method (FGSM) [12], which perturbs inputs to maximise an error metric. We first use kernel density estimation [16] with a Gaussian kernel to synthesise new ID inputs. Next, the FGSM perturbs them to increase the reconstruction error of the auto-associative reference detector from Section III. As the FGSM thus has access to the ideal error gradients, we evaluate its best-case performance. Figure 4 shows that the FGSM with a constant perturbation step size produces crisp but overly conservative OOD detection for all toy examples. In Figure 5,

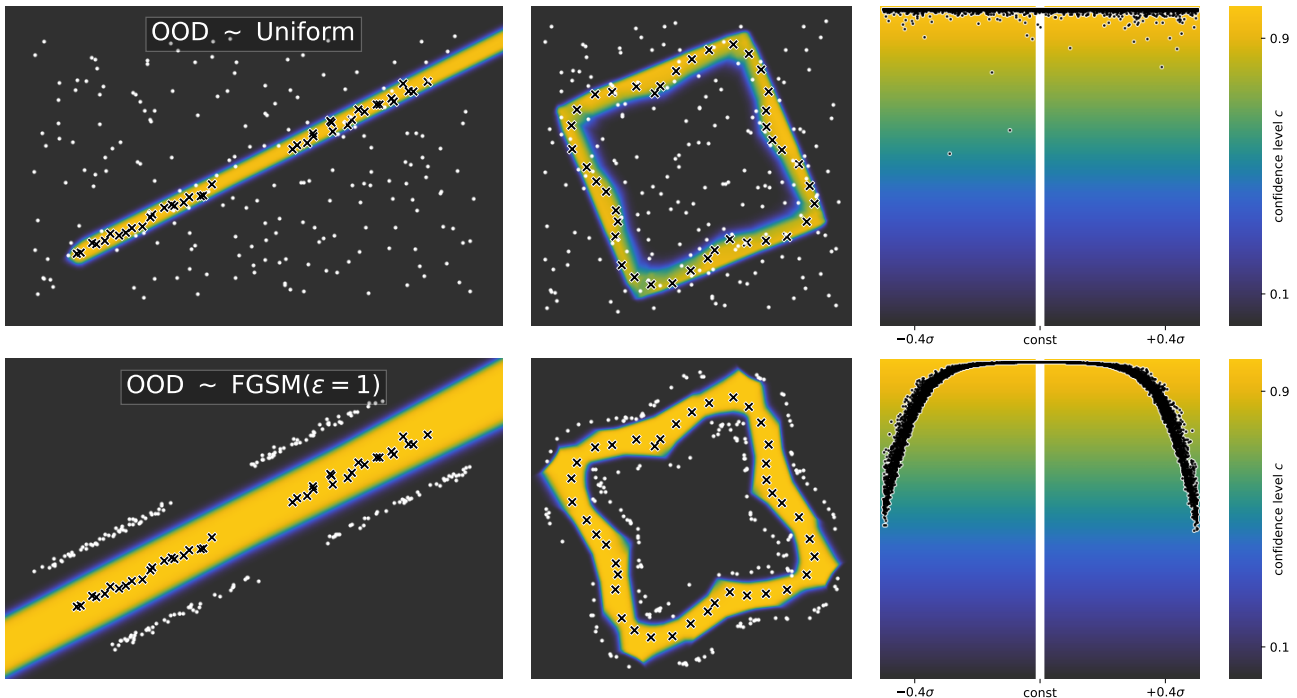


Figure 4. Comparison of supervised OOD detectors using uniform samples and FGSM with a constant step length as OOD synthesis methods.

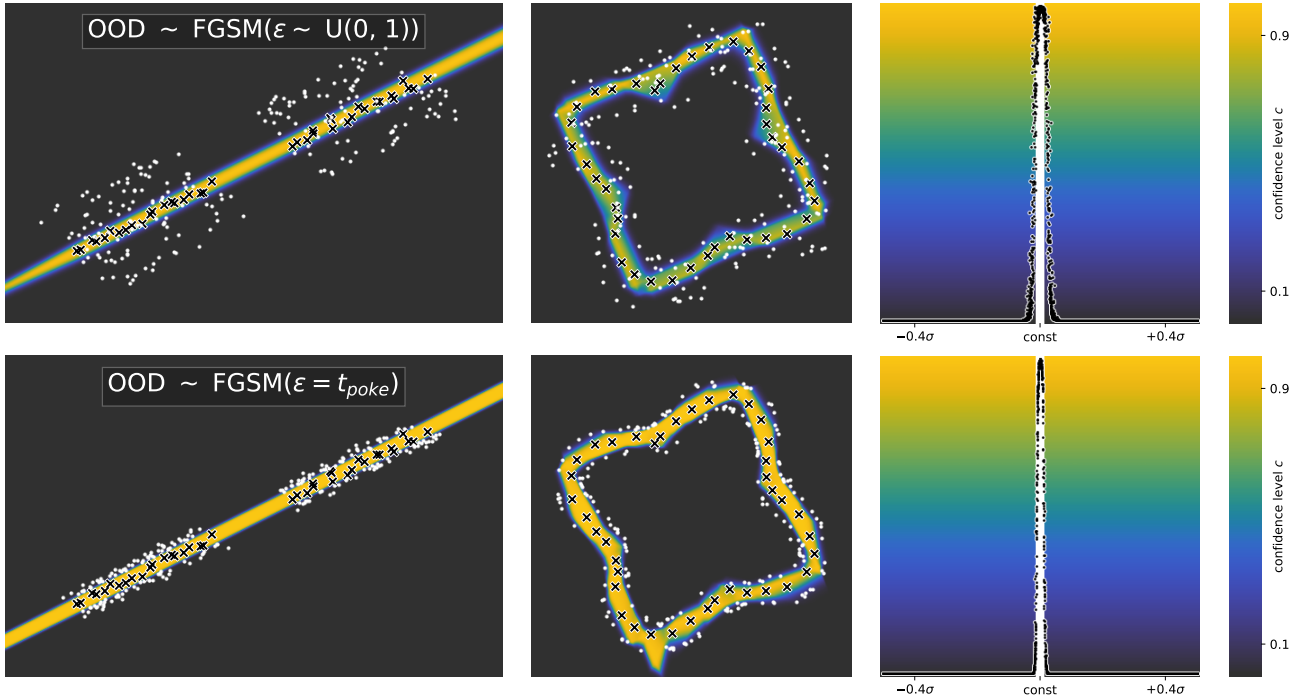


Figure 5. Comparison of supervised OOD detectors using inputs synthesised with FGSM with uniformly sampled and t -poking-determined step lengths.

sampling the step size from a distribution tightens but also blurs the boundaries as more ID-OD overlap now occurs.

is gradually adjusted to ensure that t converges. The second row in Figure 5 shows that t -poking finds a balanced step size and pushes the OOD samples very close to the ID boundary.

It is clearly beneficial to choose a FGSM step length which tightens the OOD boundary without impacting the confidence in ID inputs. Since manual tuning would be laborious, we introduce t -poking, which sets the step size to a new parameter or distribution t . After every batch, epoch or training cycle, the detector is evaluated using criteria such as “the mean confidence score for ID inputs should not fall below 0.95”. If the evaluation fails, t is multiplied by a back-off factor > 1 . Otherwise, t is multiplied by a poking factor < 1 . This factor

A. Weighting Synthetic OOD Samples in Detector Training

Overlapping ID and synthetic OOD points cannot be solved with clever OOD synthesis alone. For instance, applying an OOD synthesiser to an entirely ID parameter space would still produce synthetic OOD samples, even though they are guaranteed to be ID. This issue motivates us to define a weighting function $w_{\text{OOD}}(X) \in [0.0; 1.0]$ that weighs down OOD inputs that clash with ID training data. We assume that

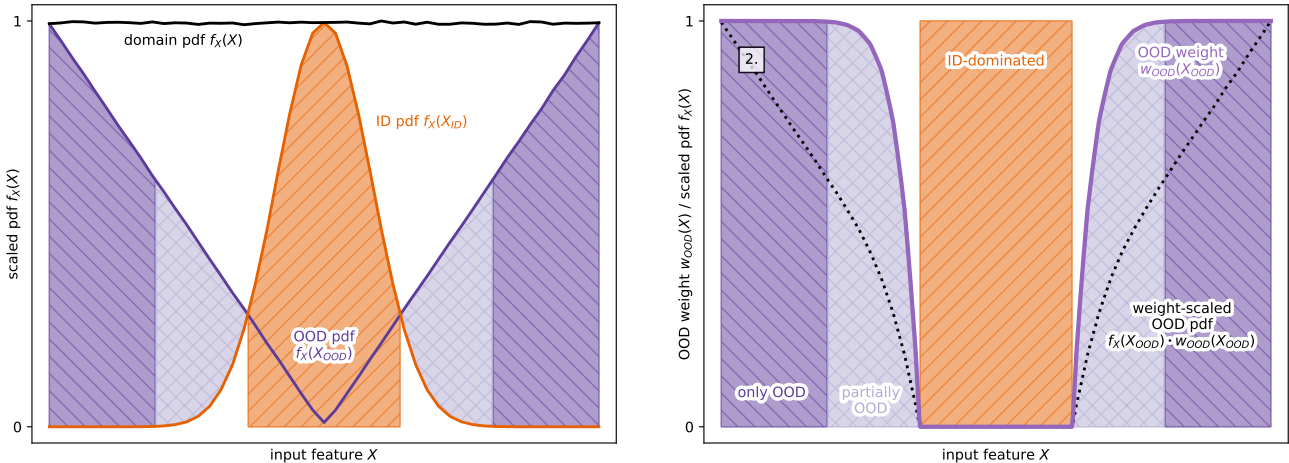


Figure 6. Example of the OOD sample down-weighting. Where ID samples dominate the input domain, shown in orange stripes, OOD samples are given zero weight to avoid ID-OD overlap. In contrast, areas without ID samples, shown in purple, are assigned full OOD weight.

there is a distribution \mathbb{P}_X of semantically valid input features that is a superset of the ID and OOD distributions. Since the synthetic OOD inputs may contain some misclassified ID inputs, we want to prioritise ID samples over synthetic OOD samples. Thus, after the ID inputs have been drawn from \mathbb{P}_X , they partially block off parts of the distribution. When synthetic OOD inputs are generated, samples that fall within ID areas are blocked and weighted down. Figure 6 shows a simple example which we use to walk through how we design

the OOD sample weight factor $w_{\text{OOD}}(X)$.

We first need to calculate the probability density functions (pdf) of the input domain distribution \mathbb{P}_X , the in-distribution $\mathbb{P}_{X_{\text{ID}}}$ and the out-of-distribution $\mathbb{P}_{X_{\text{OOD}}}$. If their analytical forms are unknown, they can be proxied, e.g. with distribution fitting or a lower-dimensional auto-associative reconstruction error.

While the ID and the OOD samples both come from the input domain, they have likely sampled it with bias. To make

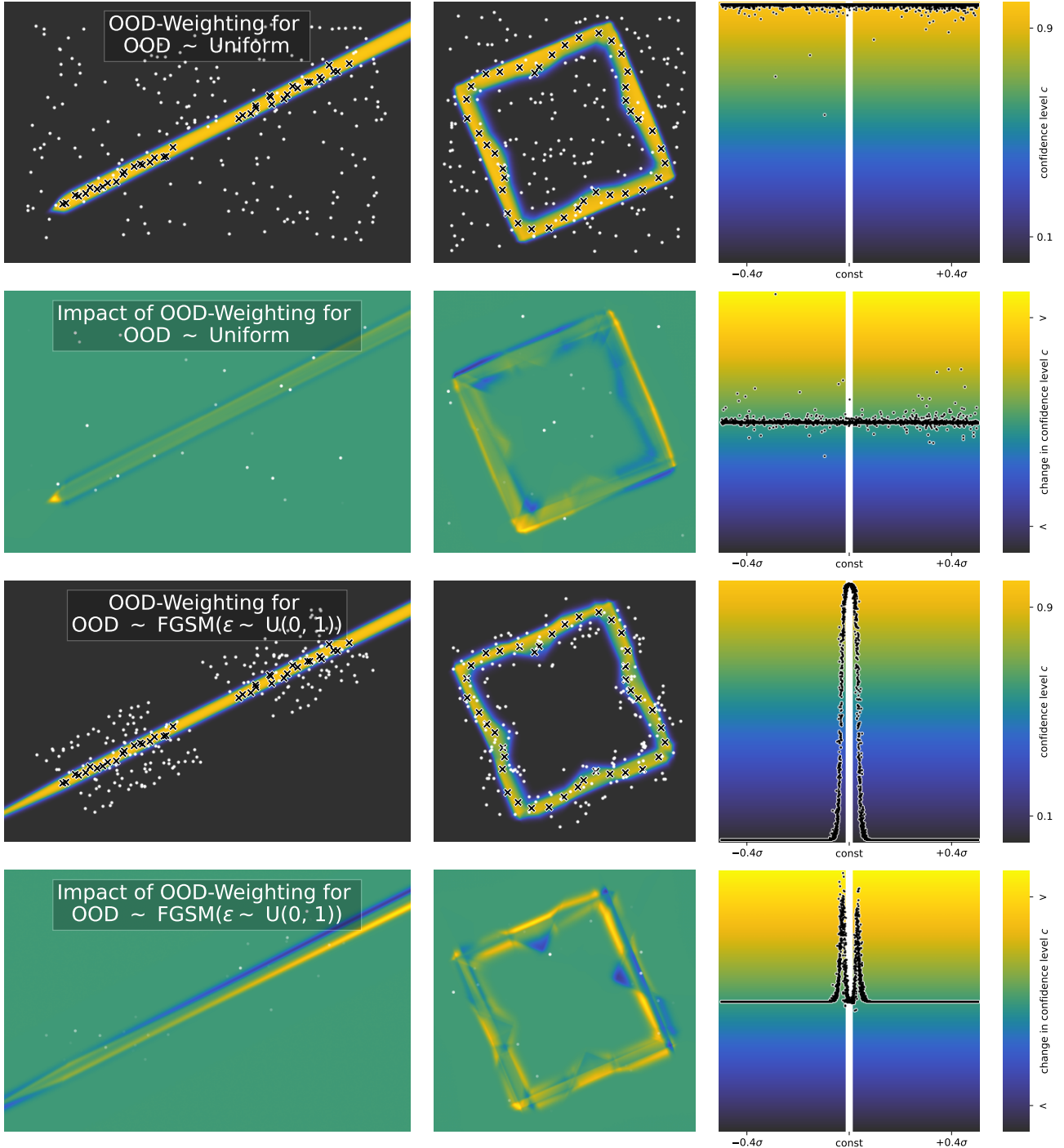


Figure 7. Evaluation of the OOD weighting scheme for uniformly (first and second row) and adversarially sampled (third and fourth row) OOD inputs. Every second row shows the difference compared to Figure 4a and Figure 5a, and encodes the ID weight of the synthetic OOD points using transparency.

Table II
 QUANTITATIVE EVALUATION OF THE DETECTION, RUNTIME, AND MEMORY PERFORMANCE OF THE OOD SYNTHESISERS FROM FIGURES 4 TO 7.

OOD Synthesiser Toy Example	Precision	F ₁ Score	ROC-AUC	Fitting Time [s]	Scoring Time [s]	Memory [kiB]
	L / C / H	L / C / H	L / C / H	L / C / H	L / C / H	L / C / H
4a Uniform	0.702 / 0.316 / 0.01	0.751 / 0.46 / 0.02	0.973 / 0.964 / 0.547	47.7 / 119 / 26.0	2.12 / 4.21 / 0.0	178 / 186 / 819
4b FGSM(1.0)	0.26 / 0.242 / 0.011	0.412 / 0.389 / 0.021	0.997 / 0.963 / 0.982	63.6 / 378 / 7e3	1.32 / 2.6 / 0.11	175 / 188 / 819
5a FGSM(U(0,1))	0.81 / 0.383 / 0.174	0.83 / 0.512 / 0.297	1.0 / 0.979 / 0.993	56.8 / 559 / 9e3	1.97 / 2.54 / 0.14	177 / 197 / 825
5b FGSM(t_{poke})	0.914 / 0.393 / 0.289	0.935 / 0.555 / 0.448	1.0 / 0.974 / 0.999	3e3 / 11e3 / 12e3	16.9 / 9.79 / 0.04	179 / 226 / 840
7a w(Uniform)	0.719 / 0.321 / 0.01	0.777 / 0.471 / 0.02	0.981 / 0.964 / 0.548	334 / 696 / 134	28.5 / 36.6 / 0.1	406 / 412 / 2e3
7c w(FGSM(U))	0.819 / 0.352 / 0.123	0.842 / 0.488 / 0.219	0.999 / 0.976 / 0.994	145 / 711 / 8e3	2.2 / 14.1 / 0.14	408 / 420 / 2e3

apparent which areas of the input domain have already been sampled, we rescale all three pdfs such that the input data pdf dominates both the ID and OOD pdfs, as seen in Figure 6.1.

Note that some of the areas have been sampled twice, i.e. the ID pdf and the OOD pdf overlap. Since we prioritise ID samples, we ignore the area below the OOD pdf wherever it overlaps with the area below the ID pdf curve.

Finally, we can calculate the weighting factor for ID and OOD samples. For any input $x \in X$, we look at the fraction of the area under the combined sampling curves, the maximum of $f_{ID}(X)$ and $f_{OOD}(X)$, that is taken up by ID to calculate the ID sample weight. The OOD sample weight $w_{OOD}(X)$ then is its complement:

$$w_{OOD}(X) = 1 - \frac{f_{ID}(X)}{\max(f_{ID}(X), f_{OOD}(X))}$$

We now evaluate the impact of applying the OOD sample weighting scheme. For simplicity, we assume that $\mathbb{P}_X = \mathbb{P}_{X_{OOD}}$ for the uniform and -FGSM methods, i.e. that OOD samples are drawn with some uniformity from the input domain distribution. The first two rows in Figure 7 show that the scheme sharpens the confidence boundaries of the uniform method by down-weighting overlapping OOD inputs, though without any clear impact on the haystack. The third and fourth rows highlight that the weighting scheme de-smudges the FGSM-based OOD boundary. However, the haystack toy example also demonstrates a case in which the weighting can result in less tight boundaries. In particular, we use kernel density estimation with a linear kernel to approximate the distribution of the reconstruction errors of the reference detector from Section III. Unfortunately, the fixed kernel bandwidth produces an overly smooth pdf approximation that is insufficient for the haystack example with a strict ID-OOD boundary.

In addition to the aforementioned qualitative evaluation, we have also scored each OOD synthesiser quantitatively, following the analysis in Section III. Table II shows that the FGSM with t -poking and the much cheaper uniformly distributed step sizes outperforms the other approaches. While all of the methods detect OOD inputs very efficiently, the supervised methods require significantly more time for fitting than the unsupervised approaches in Table I. Note that the excessively high fitting time of the FGSM is likely more indicative of our slow gradient calculation code than the method itself.

From our investigation of supervised OOD detectors using

various OOD synthesis methods in this section, we come to the following recommendations for synthesising OOD inputs:

- 1) Supervised ID-OOD detectors using synthetic OOD samples identify sharper OOD boundaries with higher ROC-AUC scores than Section III’s unsupervised methods. However, since they produce larger high-confidence areas to include most ID samples within them, they are less precise at detecting OOD inputs near the boundary.
- 2) The OOD sample down-weighting can help with underconfident ID areas and overconfident smears into OOD areas, which are caused by synthetic OOD samples that overlap ID inputs. However, the method requires access to the (approximate) pdfs of ID and OOD samples.
- 3) Adversarial OOD samples perform best but need tuning to select the level of aggressiveness. While t -poking avoids manual tuning by optimising for intuitive confidence requirements, sampling the FGSM step length from a distribution provides a cheaper alternative.

V. CONCLUSIONS

This paper has explored OOD detection, a critical component of safe machine learning, from several perspectives. First, Section III introduced **three toy examples** to evaluate OOD detection methods. These toy examples are designed to be easy to visualise and can thus help with exploring and explaining the performance of a particular method. We have created the open-source `phepy` Python package, with which all plots for this paper were produced, to help others use these toy examples as a standard comparison test in the future.

In Section III, we also compared a variety of unsupervised detectors with the three toy examples. We thus learned that **auto-associative methods** with the Mahalanobis distance and **Gaussian Processes** produce the most generalisable results, though the latter come with high computational costs.

Second, Section IV has examined synthesising OOD inputs to train a supervised OOD classifier. Our experiments demonstrate the power and shortfalls of simple methods such as randomly sampling OOD inputs or using the **fast gradient sign method** to generate them adversarially. Since the supervised detectors produce crisper but more conservative OOD detection boundaries, we also introduced two improvements, OOD sample weighting and t -poking, to tighten this boundary.

In this paper, we have focused on evaluating OOD detection methods. Why is improving the robustness of the correspond-

ing prediction model generally insufficient? Data augmentation and transfer learning are both valuable tools to ensure that a model generalises to more inputs. However, every trained model has limits and should thus be accompanied by an OOD detector to ensure its predictions can be trusted.

ACKNOWLEDGEMENTS

The authors wish to acknowledge the IT for Science Group at the University of Helsinki for computational resources.

REFERENCES

- [1] S. Pei, X. Zhang, B. Fan and G. Meng, ‘Out-of-distribution detection with boundary aware learning,’ 2021. DOI: 10.48550/arXiv.2112.11648.
- [2] J. Lu, A. Liu, F. Dong, F. Gu, J. Gama and G. Zhang, ‘Learning under concept drift: A review,’ *IEEE Transactions on Knowledge and Data Engineering*, vol. 31, no. 12, pp. 2346–2363, 2019. DOI: 10.1109/TKDE.2018.2876857.
- [3] M. G. Kim, ‘Multivariate outliers and decompositions of mahalanobis distance,’ *Communications in Statistics – Theory and Methods*, vol. 29, no. 7, pp. 1511–1526, 2000. DOI: 10.1080/03610920008832559.
- [4] R. Sjögren and J. Trygg, *Out-of-distribution example detection in deep neural networks using distance to modelled embedding*, 2021. DOI: 10.48550/arXiv.2108.10673.
- [5] M. M. Breunig, H.-P. Kriegel, R. T. Ng and J. Sander, ‘Lof: Identifying density-based local outliers,’ in *Proceedings of SIGMOD’00*, 2000, pp. 93–104. DOI: 10.1145/342009.335388.
- [6] D. Miljković, ‘Novelty detection in machine vibration data based on cluster intraset distance,’ 2008, pp. 59–66. [Online]. Available: https://www.researchgate.net/publication/304082527_Novelty_Detection_In_Machine_Vibration_Data_Based_On_Cluster_Intraset_Distance (visited on 15/01/2023).
- [7] H. Sohn, K. Worden and C. R. Farrar, ‘Novelty detection using auto-associative neural network,’ ser. IMECE, 2001, pp. 573–580. DOI: 10.1115/IMECE2001/DSC-24571.
- [8] G. Cybenko, ‘Approximation by superpositions of a sigmoidal function,’ *Math. Control. Signals, Syst.*, vol. 2, no. 4, pp. 303–314, 1989. DOI: 10.1007/BF02551274.
- [9] Y. Gal and Z. Ghahramani, ‘Dropout as a bayesian approximation: Representing model uncertainty in deep learning,’ in *Proceedings of The 33rd International Conference on Machine Learning*, M. F. Balcan and K. Q. Weinberger, Eds., vol. 48, Proceedings of Machine Learning Research, 2016, pp. 1050–1059. [Online]. Available: <https://proceedings.mlr.press/v48/gal16.html> (visited on 29/06/2023).
- [10] B. Lakshminarayanan, A. Pritzel and C. Blundell, ‘Simple and scalable predictive uncertainty estimation using deep ensembles,’ in *Proceedings of the 31st International Conference on Neural Information Processing Systems*, ser. NIPS’17, Curran Associates Inc., 2017, pp. 6405–6416. [Online]. Available: <https://dl.acm.org/doi/10.5555/3295222.3295387> (visited on 10/04/2023).
- [11] D. Hafner, D. Tran, T. Lillicrap, A. Irpan and J. Davidson, ‘Noise contrastive priors for functional uncertainty,’ 2019. DOI: 10.48550/arXiv.1807.09289.
- [12] I. J. Goodfellow, J. Shlens and C. Szegedy, *Explaining and harnessing adversarial examples*, 2014. DOI: 10.48550/arXiv.1412.6572.
- [13] K. Lee, H. Lee, K. Lee and J. Shin, *Training confidence-calibrated classifiers for detecting out-of-distribution samples*, 2017. DOI: 10.48550/arXiv.1711.09325.
- [14] P. Kovesi, *Good colour maps: How to design them*, 2015. DOI: 10.48550/arXiv.1509.03700.
- [15] F. Pedregosa, G. Varoquaux, A. Gramfort *et al.*, ‘Scikit-learn: Machine learning in python,’ *JMLR*, vol. 12, no. 85, pp. 2825–2830, 2011. [Online]. Available: <http://jmlr.org/papers/v12/pedregosa11a.html> (visited on 29/06/2023).
- [16] M. Rosenblatt, ‘Remarks on Some Nonparametric Estimates of a Density Function,’ *The Annals of Mathematical Statistics*, vol. 27, no. 3, pp. 832–837, 1956. DOI: 10.1214/aoms/1177728190.

Juniper Tyree is a doctoral student in Atmospheric Science at the University of Helsinki’s Institute for Atmospheric and Earth System Research (INAR). They use their background in computer science to support computational ecology and climate science with efficient and highly parallelisable model algorithms, accessible data analysis tooling, and data compression.

Andreas Rupp is an assistant professor at LUT’s School of Engineering Sciences. His research centres around numerical methods for partial differential equations. He tries to extend these methods to applications on graphs and hypergraphs and, ultimately, implements them in machine learning research.

Petri S. Clusius is a doctoral student in Atmospheric Science at INAR. He develops atmospheric new particle formation models and studies the role of biogenic hydrocarbons emitted from forests to future climate warming.

Michael H. Boy is a professor in Atmospheric Science and Applied Mathematics at INAR and LUT’s Department of Computational Engineering. His scientific interests are in atmospheric chemistry and aerosol dynamics, and how to apply machine learning techniques in these areas.